

Separation of dwarf and giant stars with ROTSE–IIIId

S. BILIR, T. GÜVER, and M. ASLAN

Istanbul University Science Faculty, Department of Astronomy and Space Sciences, 34119, University-Istanbul, Turkey

Abstract. 136 stars which were known to be the members of open cluster NGC 752 were observed at R band with ROTSE–IIIId telescope located at the Turkish National Observatory (TUG) site. The data had been evaluated together with BV and 2MASS photometric data. A new practical method for separating dwarf and giant was described and applied. Evaluating the colour magnitude–diagrams with Padova isochrones revealed metallicity similar to the Sun and an age of 1.41 Gyr for the open cluster NGC 752.

Key words: Galaxy: open cluster and associations, stars: colour-magnitude diagrams, stars: giants

1. Introduction

One of the problems of the Galactic astronomy is the estimation of Galactic model parameters of giant stars in our Galaxy. In many studies, the Galactic model parameters are estimated without any discrimination between dwarfs and giants, whereas some researchers estimated model parameters only for certain star categories (e.g. Pritchett 1983, Bahcall & Soneira 1984, Buser & Kaeser 1985 and Mendez & Altena 1996). A very recent work is an example for this where the Galactic model parameters were estimated using only giants (Cabrera-Lavers, Garzon & Hammersley 2005). The separation of field dwarfs and field giants plays an important role for such kinds of works. The most efficient classical methods of identifying dwarf and giant stars utilize spectroscopy. By inspecting spectral line profiles, one has to estimate surface gravity to discriminate between higher and lower pressure stellar atmospheres to be sure for the identification. This is, however time consuming and tiring. A rather easier procedure is to separate dwarfs and evolved stars (subgiants or giants) such as to obtain a luminosity function consistent with the local luminosity function of nearby stars due to Gliese & Jahreiss (1991) and Jahreiss & Wielen (1997). The procedure of this separation is based on the fact that the local luminosity functions obtained for many fields indicates a systematic excess of star counts relative to the luminosity function of nearby stars for the fainter segment, i.e. $M(V) \geq 5^m.5$, and a deficit for brighter segment, $M(V) < 5^m.5$. (in RGU system $M(G) \geq 6^m$ and $M(G) < 6^m$, respectively). The works of Karaali (1992); Ak, Karaali & Buser (1998); Karataş, Bilir & Karaali (2000); Karaali et al. (2000); Karataş, Karaali & Buser (2001); Karaali, Bilir & Buser (2004); Bilir, Karaali &

Buser (2004) and Karataş et al. (2004) can be given as examples for application of this procedure.

Recently, a new method were suggested by Bilir et al. (2006) for separating the field dwarfs and field giants. This new method is based on the comparison of the Two Micron All Sky Survey (2MASS, hereafter) J , H , K_s with the V magnitudes down to the limiting magnitude of $V = 16$. In this work we extend application of this method to the open cluster NGC 752 observed by a robotic telescope ROTSE–IIIId (Akerlof et al. 2003).

This paper is organized as follows. In Section 2 the BV, 2MASS and ROTSE data are presented. In Section 3 the method is applied to ROTSE and 2MASS data, and the separation of dwarf and giant stars is tested. In Section 4 colour-magnitude diagrams (CMDs) of NGC 752 is compared to the Padova isochrones. Finally, the conclusion is given in Section 5.

2. Observations

2.1. The BV and 2MASS Data

NGC 752=C0154+374 ($\alpha = 01^h 57^m 41^s$, $\delta = +37^\circ 47' 06''$; $l = 137^\circ.13$, $b = -23^\circ.25$; J2000) has been subject of many studies, because it is the nearest intermediate-age cluster, with 427 pc (Dzervitis & Paupers 1993) distance from the Sun. It is usually considered as metal-deficient with respect to the Sun, $[Fe/H] = -0.15 \pm 0.05$ dex, slightly reddened $E(B-V) = 0.035 \pm 0.005$, with distance module $(m-M) = 8.25 \pm 0.10$ (Daniel et al. 1994). Accurate proper motion and radial velocity measurements show that there are 136 probable member stars of the open cluster (Daniel et al. 1994). V magnitudes and $(B-V)$ colour indices used in

Correspondence to: sbilir@istanbul.edu.tr

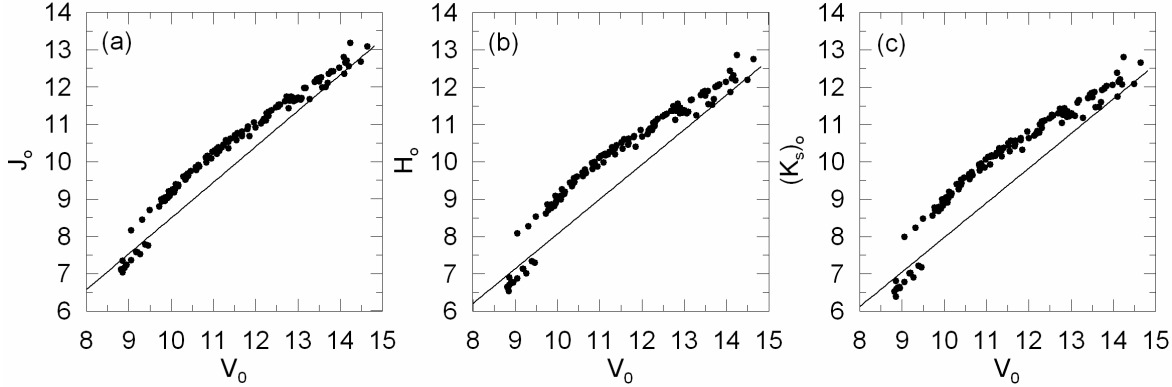


Fig. 2. V and 2MASS magnitudes of 136 stars in NGC 752. (a) $J_0 \times V_0$, (b) $H_0 \times V_0$, and (c) $(K_s)_0 \times V_0$. The solid lines in diagrams were drawn according to eqs. (1), (2), and (3).

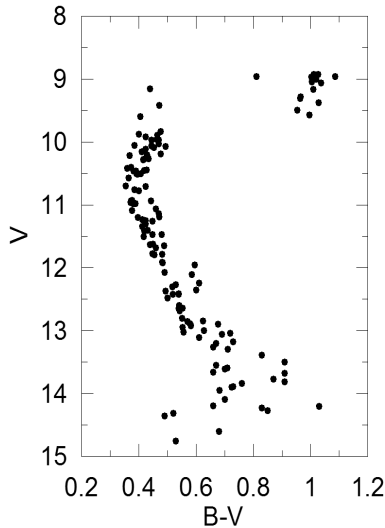


Fig. 1. $V \times (B - V)$ CMD of 136 probable member stars in NGC 752.

this study were taken from Daniel et al. (1994) and they were given in Table 1. The $V \times (B - V)$ CMD in Fig. 1 shows that stars with $V < 10$ and $(B - V) > 0.80$ are giants.

Recently the 2MASS, including the Point-Source Catalogue and Atlas, has produced huge amounts of data to be explored in the coming years (Skrutskie et al. 1997). The photometric system comprises Johnson's J ($1.25 \mu\text{m}$) and H ($1.65 \mu\text{m}$) bands with the addition of K_s ($2.17 \mu\text{m}$), slightly bluer than Johnson's K . The 2MASS sky coverage, homogeneity and depth will certainly make this set of filters a photometric standard reference for the future.

2MASS data of the 136 probable member stars in NGC 752 are obtained by Vizier¹ in CDS and they are given in Table 1. We used the equations of Fiorucci & Munari (2003) for the determination of the total absorptions for the bands V , J , H and K_s , i.e. $A(V) = 3.1E(B - V)$, $A(J) = 0.887E(B - V)$, $A(H) = 0.565E(B - V)$ and $A(K_s) = 0.382E(B - V)$. Thus the de-reddened magnitudes were obtained as follows: $V_0 = V - A(V)$, $J_0 = J - A(J)$, $H_0 = H - A(H)$

and $(K_s)_0 = K_s - A(K_s)$. The subscript "0" indicates de-reddened magnitude.

$J_0 \times V_0$, $H_0 \times V_0$ and $(K_s)_0 \times V_0$ diagrams for the cluster stars are given in Fig. 2. The solid lines represent the equations in Bilir et al. (2006), i.e.

$$J_0 = 0.957V_0 - 1.079, \quad (1)$$

$$H_0 = 0.931V_0 - 1.240, \quad (2)$$

$$(K_s)_0 = 0.927V_0 - 1.292. \quad (3)$$

14 stars below the lines are the giants in Fig. 1, whereas 122 stars above the lines are the dwarfs of the same cluster. The distribution of different star categories at different sides of the lines in three figures were presented here to confirm separation of dwarfs and giants.

2.2. ROTSE data

The Robotic Optical Transient Experiment (ROTSE-III) consists of four 0.45m worldwide robotic, automated telescopes situated at different locations on Earth. They are designed for fast (~ 6 sec) responses to Gamma-Ray Burst (GRB) triggers from satellites such as Swift. Each ROTSE telescope has a $1.85 \times 1.85 \text{ deg}^2$ field of view, and uses a Marconi 2048 \times 2048 back illuminated thinned CCD. These telescopes operate without filters, and have wide passband which peaks around 550 nm (Akerlof et al. 2003). In this work, we present optical observations of NGC 752 performed by ROTSE-IIId, telescope located at Turkish National Observatory (TUG) site, Bakırtepe, Turkey. The observations took place between MJD 53637 (September 2005) and MJD 53649 (October 2005). A total of about 217 CCD frames were analyzed. After determining the instrumental magnitudes (Bertin & Arnouts, 1996), they were reduced to ROTSE magnitudes via comparing all the field stars with the USNO A2.0 R -band catalog. All the processes were done in an automated mode.

R -band magnitudes of the 136 stars are given in Table 1. ROTSE magnitudes are also de-reddened in order to homogenize the data. The total absorption for the R band could be determined by the equation of Fiorucci & Munari (2003), i.e. $A(R) = 2.613E(B - V)$. Thus the de-reddened magnitude in R becomes $R_0 = R - A(R)$.

¹ <http://vizier.u-strasbg.fr/viz-bin/Vizier?-source=2MASS>

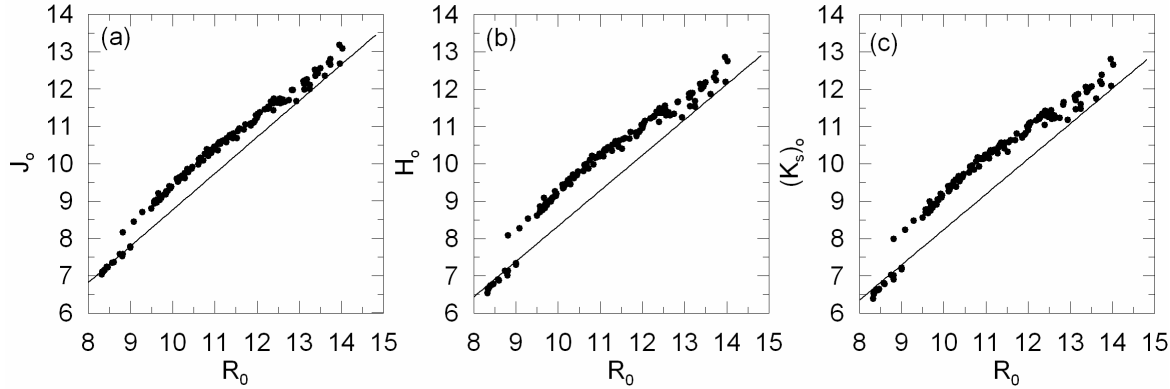


Fig. 4. R_0 and 2MASS magnitudes of 136 stars in NGC 752. (a) $J_0 \times R_0$, (b) $H_0 \times R_0$, and (c) $(K_s)_0 \times R_0$. The solid lines in diagrams were drawn according to eqs. (5), (6), and (7).

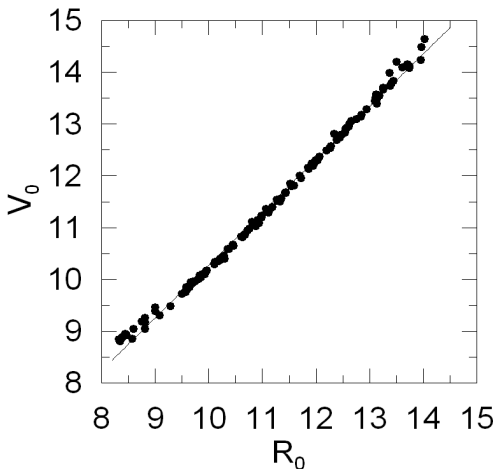


Fig. 3. $R_0 \times V_0$ magnitudes of 136 stars in NGC 752.

3. Application of the method to ROTSE-IIIId data

We used the following relation between the V_0 magnitude and the ROTSE-IIIId magnitude R_0 for 136 stars of the open cluster NGC 752 (Fig. 3) in order to apply the method to ROTSE-IIIId data:

$$V_0 = (1.019 \pm 0.006)R_0 + 0.092 \pm 0.070 \quad (\sigma = 0.10). \quad (4)$$

Thus, substituting the value of V_0 in (4) into (1), (2), and (3) we obtain the relations between 2MASS and ROTSE-IIIId magnitudes, i.e.

$$J_0 = 0.975R_0 - 0.991, \quad (5)$$

$$H_0 = 0.949R_0 - 1.154, \quad (6)$$

$$(K_s)_0 = 0.945R_0 - 1.207. \quad (7)$$

The diagrams $J_0 \times R_0$, $H_0 \times R_0$ and $(K_s)_0 \times R_0$ for the NGC 752 cluster stars and the line corresponding to the eqs. (5), (6), and (7) are given in Fig. 4. One can see that dwarfs and giants lie at opposite sides of the line in these figures, especially the relation between $(K_s)_0 \times R_0$ (Fig. 4c) is the most successful in separating of the two different star categories.

4. Age estimation for the open cluster NGC 752 via two photometries

We estimated the age of the open cluster NGC 752 by the means of BV and 2MASS data to show the advantage. The absolute magnitudes of the stars were determined by the corresponding apparent magnitudes and the distance module of the cluster. The Padova isochrones were taken from Girardi et al. (2002) and Bonatto, Bica & Girardi (2004) for BV² and 2MASS³ photometry, respectively. The isochrone sets were computed with updated opacities, and equations of state, and a moderate amount of convective overshoot. The basic isochrone set presented in Girardi et al. (2002) covers a very wide range of initial masses (from 0.15 to $\sim 100M_\odot$), metallicities, and photometric systems, being well suited for studies of all ages.

The isochrones mentioned above were fitted to the CMDs in Figs. 5-7 for two sets of chemical compositions, i.e. Z=0.019, Y=0.273 (panel a) and Z=0.008, Y=0.250 (panel b). The isochrones in Fig. 5a fits to the main-sequence and turn-off segments of the $M_V \times (B-V)_0$ diagram and reveal an age of $t = 1.26$ Gyr, whereas in Fig. 5b, the isochrones could be fitted only to the giant branch of the same CMD, resulting a larger age, i.e. $t = 1.78$ Gyr. The isochrones could not be fitted to all segments of the $M_J \times (J-H)_0$ diagram in Fig. 6 either. In Fig. 6a the fit is better to the main-sequence and turn-off segments, however it is only to the giant branch in Fig. 6b. The best fit is accomplished with the isochrone of age $t = 1.41$ Gyr to the $M_J \times (J-K_s)_0$ in Fig. 7a. In fact, the isochrone fits to all segments, main-sequence, turn-off and giant branch, for a metallicity close to the solar one which is expected (Daniel et al. 1994). Thus, the comparison of the six diagrams in Figs. 5-7 reveals that the CMD $M_J \times (J-K_s)_0$ is the best one which fits for the age estimation.

² http://pleiadi.pd.astro.it/isoc_photsys.02/isoc_photsys.02.html

³ http://pleiadi.pd.astro.it/isoc_photsys.01/isoc_2mass/index.html

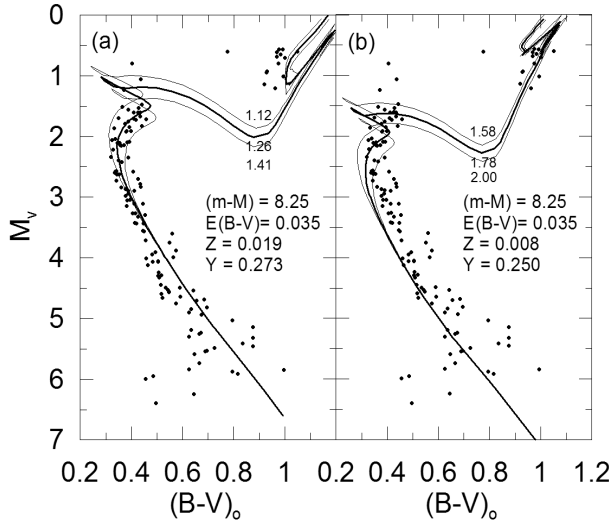


Fig. 5. $M_V \times (B-V)_0$ CMDs of NGC 752. (a) $Z=0.019$ and 1.12, 1.26 and 1.41 Gyr and (b) $Z=0.008$ and 1.58, 1.78 and 2.00 Gyr of Padova isochrones.

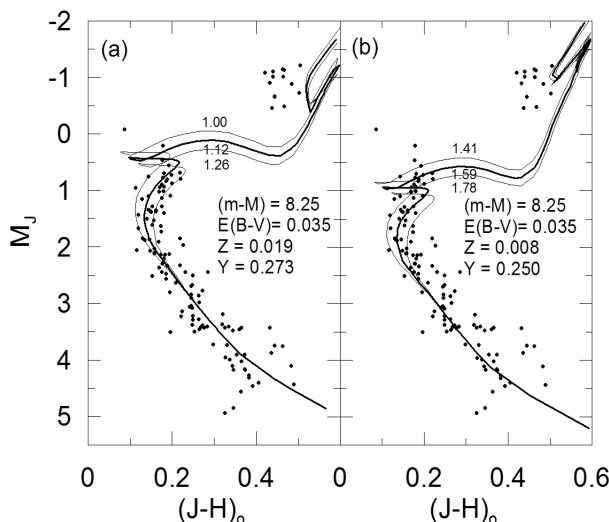


Fig. 6. $M_J \times (J-H)_0$ CMDs of NGC 752. (a) $Z=0.019$ and 1.00, 1.12 and 1.26 Gyr and (b) $Z=0.008$ and 1.41, 1.59 and 1.78 Gyr of Padova isochrones.

5. Conclusion

In this study, we have reduced the relations between the 2MASS and V magnitudes by which field dwarfs and giants can be separated, to the USNO A2.0 R -band magnitudes. The R_0 magnitudes of 136 stars in open cluster NGC 752 were transferred to the V_0 magnitudes, and the relations between J_0 , H_0 , $(K_s)_0$ and R_0 were derived by means of the relations between J_0 , H_0 , $(K_s)_0$ and V_0 given by Bilir et al. (2006). Dwarf and giant stars identified by the CMD of open cluster NGC 752 lie at different sides of the line representing the relation between the 2MASS and R_0 magnitudes, in the $J_0 \times R_0$, $H_0 \times R_0$ and $(K_s)_0 \times R_0$ diagrams. The best one is the last diagram, i.e. $(K_s)_0 \times R_0$. Thus, dwarf-giant separation could be carried out also in the ROTSE-IIId data. Proven to be successful, this practical method can provide

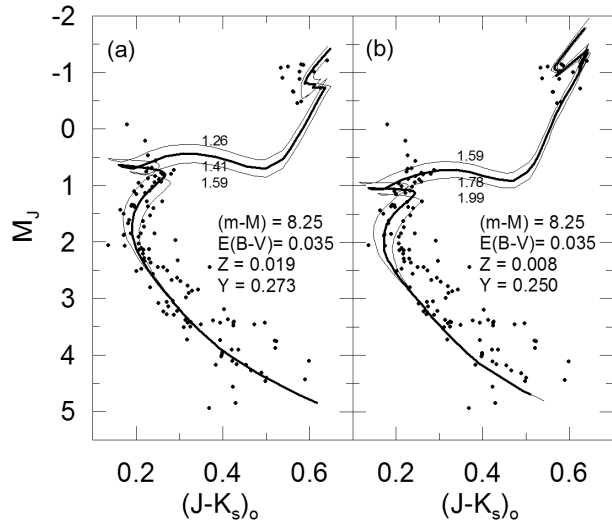


Fig. 7. $M_J \times (J-K_s)_0$ CMDs of NGC 752. (a) $Z=0.019$ and 1.26, 1.41 and 1.59 Gyr and (b) $Z=0.008$ and 1.59, 1.78 and 1.99 Gyr of Padova isochrones.

good contributions to the studies of Galactic model parameters in which separation of dwarfs and giants were needed.

A set of Padova isochrones were fitted to the CMDs of the open cluster NGC 752 using BV and 2MASS photometric data. It turned out that the isochrone with chemical composition $Z=0.019$ and $Y=0.273$ which reveals an age of 1.41 Gyr for the open cluster NGC 752 could be fitted to all segments, i.e. main-sequence, turn-off and giant branch, of the $M_J \times (J-K_s)_0$ two-colour diagram. This result is very close to the age 1.24 ± 0.20 Gyr which Salaris, Weiss & Percival (2004) calculated from the morphology of 71 open clusters in our Galaxy. The metal-abundance of the cluster given by Daniel et al. (1994), i.e. $[Fe/H] = -0.15 \pm 0.05$ dex, is a strong confirmation for our result.

Acknowledgements. We thank international ROTSE collaboration and TUG for the optical facilities (Project number: TUG-ROTSE.05.14). This research has made use of the SIMBAD database, operated at CDS, Strasbourg, France. This publication makes use of data products from the Two Micron All Sky Survey, which is a joint project of the University of Massachusetts and the Infrared Processing and Analysis Center/California Institute of Technology, funded by the National Aeronautics and Space Administration and the National Science Foundation. We would also like to thank Dr. Salih Karaali for helpful comments and suggestions, Dr. Zeki Eker for reading the whole manuscript and correction and Dr. Tansel Ak for various helps. This work was supported by the Research Fund of the University of Istanbul. Project number: BYP 914.

References

- Ak, S.G., Karaali, S., Buser, R.: 1998, A&AS, 131, 345
- Akerlof, C.W., et al.: 2003, PASP, 115, 132
- Bahcall, J.N., Soneira, R.M.: 1984, ApJS, 55, 67
- Bertin, E., Arnouts, S.: 1996, A&AS, 117, 393
- Bilir, S., Karaali, S., Buser, R.: 2004, TJPh, 28, 289
- Bilir, S., Karaali, S., Güver, T., Karataş, Y., Ak, S.: 2006, AN, 327,

- Bonatto, Ch., Bica, E., Girardi, L.: 2004, A&A, 415, 571
Buser, R., Kaeser, U.: 1985, A&A, 145, 1
Cabrera-Lavers, A., Garzon, F., Hammersley, P.L.: 2005, A&A, 433,
173
Daniel, S.A., Latham, D.W., Mathieu, R.D., Twarog, B.A.: 1994,
PASP, 106, 281
Dzervitis, U., Paupers, O.: 1993, Ap&SS, 199, 77
Fiorucci, M., Munari, U.: 2003, A&A, 401, 781
Girardi, L., Bertelli, G., Bressan, A., Chiosi, C., Groenewegen,
M.A.T., Marigo, P., Salasnich, B., Weiss, A.: 2002, A&A, 391,
195
Gliese, W., Jahreiss, H.: 1991, Preliminary Version of the Third Cat-
alogue of Nearby Stars, Astron. Rechen-Institut, Heidelberg
Jahreiss, H., Wielen, R.: 1997, ESASP 402, 675, eds. Battick, B.,
Perryman, M.A.C., & Bernacca, P.L.
Karaali, S.: 1992, VIII. Nat. Astron. Symp. Eds. Z. Aslan and O.
Gölbaşı, Ankara-Turkey, p.202
Karaali, S., Karataş, Y., Bilir, S., Ak, S.G., Gilmore, G.: 2000, The
Galactic Halo: From Globular Cluster to Field Stars, Proceed-
ings of the 35th Liege International Astrophysics Colloquium,
353
Karaali, S., Bilir, S., Buser, R.: 2004, PASA, 21, 275
Karataş, Y., Bilir, S., Karaali, S.: 2000, The Galactic Halo: From
Globular Cluster to Field Stars, Proceedings of the 35th Liege
International Astrophysics Colloquium, 407
Karataş, Y., Karaali, S., Buser, R.: 2001, A&A, 373, 895
Karataş, Y., Bilir, S., Karaali, S., Ak, S.G.: 2004, AN, 325, 726
Mendez, R.A., van Altena, W.F.: 1996, AJ, 112, 655
Pritchett, C.: 1983, AJ, 88, 1476
Salaris, M., Weiss, A., Percival, S. M.: 2004, A&A, 414, 163
Skrutskie, M.F., et al.: 1997, The Impact of Large-Scale Near-IR
Sky Surveys, ed. F. N. Epcstein, A. Omont, B. Burton, & P.
Persei Garzon, (Dordrecht: Kluwer), 210, 187

Table 1. BV, ROTSE and 2MASS magnitudes and its errors of 136 probable member stars of open cluster NGC 752. ID name is the same as Daniel et al. (1994) and the coordinates are for the epoch 2000.

ID	α	δ	V	B-V	R	J	H	K_s
143	01 54 31.04	+37 29 31.6	11.140	0.470	10.970	0.010	10.343	0.019
215	01 54 56.71	+37 58 28.9	11.400	0.430	11.200	0.012	10.615	0.021
222	01 54 59.65	+37 28 59.8	11.651	0.009	0.489	0.007	11.365	0.011
237	01 55 02.85	+38 16 38.1	12.418	0.000	0.519	0.000	12.110	0.017
245	01 55 07.13	+37 32 36.9	14.190	0.660	13.830	0.026	12.838	0.022
259	01 55 12.62	+37 50 14.4	9.496	0.013	0.954	0.006	9.092	0.016
264	01 55 15.29	+37 50 31.2	9.569	0.005	0.996	0.003	9.090	0.017
300	01 55 26.18	+38 08 22.0	13.610	0.700	13.200	0.019	12.182	0.018
305	01 55 27.68	+37 34 04.5	10.152	0.003	0.411	0.001	9.940	0.011
308	01 55 27.67	+37 59 55.2	9.285	0.011	0.966	0.009	8.902	0.020
313	01 55 29.29	+37 50 26.2	9.968	0.013	0.470	0.001	9.718	0.014
350	01 55 39.37	+37 52 52.4	8.922	0.002	1.011	0.006	8.439	0.024
356	01 55 42.39	+37 37 54.3	9.161	0.003	1.010	0.001	8.687	0.020
361	01 55 44.75	+37 54 42.5	13.899	0.000	0.724	0.000	13.497	0.025
363	01 55 44.93	+38 08 21.4	10.420	0.360	10.189	0.013	9.619	0.021
372	01 55 47.40	+37 42 26.4	9.890	0.005	0.464	0.000	9.656	0.011
391	01 55 53.54	+37 49 26.6	13.890	0.730	13.501	0.024	12.457	0.023
397	01 55 55.53	+37 28 33.2	9.831	0.000	0.477	0.005	9.585	0.011
413	01 55 59.44	+37 40 48.5	12.303	0.016	0.517	0.022	12.035	0.013
429	01 56 02.95	+37 36 32.7	14.270	0.850	13.791	0.033	12.741	0.023
435	01 56 03.69	+37 59 22.4	11.467	0.017	0.447	0.010	11.223	0.013
455	01 56 08.96	+37 39 52.6	10.512	0.013	0.395	0.003	10.298	0.020
461	01 56 10.30	+37 44 59.9	10.054	0.002	0.384	0.006	9.752	0.041
465	01 56 11.11	+37 45 11.1	11.229	0.012	0.412	0.007	10.896	0.045
472	01 56 12.88	+38 01 43.2	11.060	0.460	10.813	0.140	10.127	0.020
475	01 56 13.70	+37 15 56.9	12.847	0.000	0.624	0.000	12.496	0.016
477	01 56 13.96	+37 47 04.7	10.572	0.006	0.364	0.006	10.375	0.015
479	01 56 14.28	+37 58 14.2	10.938	0.011	0.442	0.005	10.696	0.014
486	01 56 15.51	+37 38 41.5	10.074	0.000	0.493	0.006	9.824	0.012
505	01 56 18.63	+37 37 39.3	10.778	0.005	0.399	0.008	10.543	0.014
506	01 56 18.90	+37 58 00.4	8.971	0.018	1.003	0.011	8.456	0.044
512	01 56 21.65	+37 36 08.2	9.375	0.022	1.029	0.004	8.896	0.018
517	01 56 22.57	+37 39 17.8	14.230	0.830	13.833	0.030	12.681	0.021
520	01 56 23.10	+37 38 03.0	12.850	0.570	12.530	0.016	11.684	0.021
542	01 56 29.45	+37 55 14.7	14.350	0.490	14.045	0.032	13.214	0.024
552	01 56 32.05	+37 34 22.2	12.921	0.016	0.581	0.036	12.425	0.025
555	01 56 32.96	+37 56 46.4	11.786	0.001	0.482	0.006	11.514	0.014
563	01 56 34.46	+38 08 49.4	13.680	0.910	13.216	0.020	12.020	0.019
575	01 56 36.88	+37 45 12.7	13.840	0.760	13.477	0.029	12.384	0.020
580	01 56 39.22	+37 51 41.1	10.398	0.007	0.373	0.005	10.194	0.015
619	01 56 47.60	+37 24 30.4	10.280	0.022	0.415	0.005	10.054	0.013
622	01 56 48.61	+37 29 11.2	10.503	0.001	0.391	0.007	10.321	0.013
626	01 56 49.77	+38 01 21.7	9.158	0.016	0.439	0.006	8.902	0.032
630	01 56 50.44	+38 01 58.1	8.961	0.011	0.811	0.020	8.661	0.059
641	01 56 53.06	+37 52 09.3	10.270	0.004	0.434	0.004	10.036	0.014
648	01 56 54.33	+37 23 51.9	12.108	0.000	0.585	0.000	11.782	0.014
653	01 56 55.38	+38 04 45.8	12.410	0.540	12.088	0.013	11.262	0.019
654	01 56 55.77	+37 47 59.3	11.196	0.000	0.396	0.014	11.022	0.015
655	01 56 56.15	+38 08 16.2	13.040	0.720	12.665	0.017	11.706	0.021
659	01 56 56.35	+37 39 51.3	10.116	0.003	0.424	0.001	9.898	0.014
667	01 56 57.59	+37 23 20.5	10.925	0.021	0.377	0.004	10.720	0.170
682	01 57 02.51	+37 53 07.7	11.255	0.012	0.447	0.002	11.007	0.014
684	01 57 02.81	+38 14 03.5	12.480	0.500	12.153	0.015	11.415	0.021
687	01 57 03.12	+38 08 02.6	8.927	0.002	1.026	0.004	8.424	0.024
689	01 57 03.19	+37 55 44.5	11.788	0.005	0.455	0.009	11.529	0.015
694	01 57 03.64	+38 05 11.7	11.779	0.011	0.448	0.007	11.520	0.013
699	01 57 04.89	+38 07 33.1	13.001	0.024	0.627	0.048	12.647	0.016
701	01 57 05.47	+37 50 42.8	13.060	0.690	12.700	0.017	11.684	0.019
720	01 57 10.50	+38 02 06.6	12.367	0.020	0.494	0.034	12.064	0.013
722	01 57 10.35	+37 25 55.3	13.500	0.910	13.221	0.021	12.178	0.019
723	01 57 10.53	+37 27 26.6	13.770	0.870	13.339	0.033	12.030	0.019
728	01 57 12.13	+37 59 24.8	9.420	0.005	0.471	0.004	9.169	0.011
731	01 57 12.17	+37 56 04.7	11.956	0.000	0.595	0.000	11.608	0.013
745	01 57 14.27	+37 46 51.0	9.874	0.011	0.400	0.007	9.659	0.016
756	01 57 17.11	+37 26 08.8	10.207	0.012	0.428	0.004	9.971	0.013
768	01 57 19.42	+37 59 23.5	12.072	0.011	0.490	0.000	11.811	0.014
772	01 57 20.73	+37 51 43.1	10.188	0.009	0.476	0.003	9.923	0.012
783	01 57 22.29	+37 36 23.2	12.240	0.610	11.946	0.015	11.054	0.018
786	01 57 22.97	+37 38 21.8	13.170	0.730	12.746	0.016	11.703	0.018
790	01 57 23.81	+37 52 11.9	12.267	0.012	0.529	0.018	11.938	0.015
							11.117	0.018
							10.860	0.019
							10.756	0.018

ID	α	δ	V	B-V	R	J	H	K_s
791	01 57 24.01	+38 06 10.4	12.684	0.017	0.543	0.017	12.370	0.015
798	01 57 26.01	+37 43 19.7	10.454	0.005	0.419	0.004	10.226	0.013
799	01 57 26.17	+37 39 20.3	11.304	0.004	0.423	0.004	11.073	0.013
806	01 57 27.47	+37 35 10.4	10.756	0.000	0.385	0.000	10.555	0.015
814	01 57 28.26	+37 24 02.6	10.219	0.011	0.367	0.007	10.015	0.014
823	01 57 30.93	+37 54 57.9	10.273	0.003	0.417	0.002	10.037	0.014
824	01 57 31.86	+37 53 40.6	11.629	0.011	0.440	0.005	11.375	0.015
828	01 57 32.58	+37 42 05.8	13.943	0.000	0.681	0.000	13.537	0.024
847	01 57 35.91	+37 58 23.1	14.200		1.030		13.704	0.025
849	01 57 36.23	+37 45 10.0	9.917	0.010	0.424	0.005	9.682	0.013
857	01 57 37.69	+37 49 00.7	10.028	0.011	0.470	0.002	9.780	0.013
858	01 57 37.62	+37 39 37.8	8.958	0.003	1.085	0.004	8.416	0.030
859	01 57 37.77	+37 49 50.4	13.200		0.670		12.842	0.016
864	01 57 38.78	+38 08 30.3	12.885	0.013	0.578	0.017	12.553	0.017
867	01 57 38.97	+37 46 12.2	9.041	0.007	1.004	0.006	8.556	0.019
868	01 57 39.46	+37 52 25.8	10.465	0.014	0.381	0.005	10.262	0.014
888	01 57 43.97	+37 51 42.1	10.447	0.007	0.427	0.003	10.208	0.012
889	01 57 44.46	+38 11 06.8	12.802	0.015	0.551	0.018	12.475	0.014
890	01 57 44.74	+37 59 18.4	10.087	0.011	0.453	0.006	9.837	0.014
897	01 57 46.07	+38 04 28.4	10.506	0.037	0.407	0.003	10.382	0.170
901	01 57 47.15	+37 47 30.3	10.981	0.006	0.388	0.007	10.763	0.014
917	01 57 51.42	+37 39 52.4	14.310		0.520		13.590	0.026
921	01 57 52.00	+37 27 46.0	12.644	0.011	0.553	0.007	12.349	0.013
935	01 57 55.20	+37 52 46.0	11.620		0.450		11.417	0.014
937	01 57 54.97	+37 20 26.6	10.980		0.380		10.762	0.014
941	01 57 56.45	+37 50 01.0	10.706	0.006	0.424	0.001	10.462	0.014
950	01 57 57.79	+37 48 22.3	11.467	0.020	0.480	0.007	11.160	0.077
952	01 57 58.24	+37 26 06.4	12.650		0.540		12.356	0.014
953	01 57 58.85	+37 41 26.8	12.352	0.038	0.600	0.008	12.012	0.014
955	01 57 59.37	+37 54 53.8	9.968	0.010	0.445	0.001	9.730	0.013
964	01 58 02.79	+38 02 30.4	12.912	0.016	0.582	0.014	12.568	0.015
983	01 58 06.31	+37 38 06.6	13.110		0.610		12.709	0.017
988	01 58 07.71	+37 39 57.0	10.934	0.008	0.373	0.004	10.714	0.016
993	01 58 09.26	+37 28 35.5	13.590	0.000	0.708	0.000	13.226	0.018
999	01 58 10.66	+37 24 05.9	13.550		0.670		13.189	0.019
1000	01 58 11.43	+37 39 33.4	11.410	0.012	0.419	0.006	11.175	0.014
1003	01 58 12.27	+37 32 38.2	11.193	0.003	0.472	0.003	10.933	0.014
1007	01 58 13.40	+38 11 41.5	13.018	0.025	0.556	0.042	12.641	0.016
1008	01 58 12.71	+37 34 40.4	10.959	0.005	0.371	0.004	10.743	0.015
1012	01 58 12.94	+37 15 20.2	12.417	0.015	0.539	0.000	12.113	0.016
1017	01 58 15.33	+37 33 19.6	13.260		0.660		12.920	0.017
1023	01 58 16.88	+37 38 15.9	11.250	0.015	0.424	0.010	11.005	0.013
1026	01 58 19.00	+38 32 14.0	11.089	0.016	0.377	0.017	10.851	0.010
1027	01 58 18.42	+38 06 54.0	12.597	0.020	0.541	0.036	12.282	0.022
1083	01 58 27.61	+37 35 22.2	11.920	0.011	0.484	0.007	11.676	0.014
1089	01 58 29.84	+37 51 37.4	9.303	0.007	0.963	0.008	8.836	0.021
1107	01 58 34.42	+37 40 15.1	13.660		0.660		13.273	0.020
1117	01 58 36.91	+37 45 10.6	9.598	0.002	0.406	0.002	9.370	0.012
1123	01 58 38.12	+37 32 15.7	11.507	0.000	0.417	0.007	11.278	0.014
1129	01 58 40.07	+37 38 05.1	11.910	0.011	0.481	0.007	11.629	0.014
1151	01 58 47.96	+38 26 08.2	10.063	0.013	0.444	0.014	9.788	0.014
1161	01 58 50.00	+37 59 46.6	14.600		0.680		14.060	0.040
1165	01 58 50.44	+37 20 52.0	10.462	0.000	0.390	0.000	10.239	0.013
1172	01 58 52.93	+37 48 57.0	9.060	0.003	1.036	0.006	8.529	0.036
1178	01 58 53.94	+37 34 42.6	13.390		0.830		13.028	0.015
1196	01 58 57.32	+37 39 40.9	13.810		0.910		13.339	0.019
1204	01 58 59.87	+38 01 18.9	11.680		0.460		11.446	0.014
1263	01 59 14.82	+38 00 55.2	9.006	0.011	1.019	0.007	8.483	0.025
1270	01 59 18.04	+37 49 49.4	14.090		0.700		13.457	0.060
1284	01 59 19.91	+37 23 23.1	12.893	0.000	0.677	0.000	12.476	0.013
1296	01 59 26.08	+37 40 39.9	14.750		0.530		14.111	0.035
1304	01 59 29.63	+38 16 04.3	11.341	0.008	0.412	0.011	11.076	0.014
1365	01 59 47.27	+37 49 53.8	13.290		0.710		12.935	0.018
1407	01 59 56.83	+37 58 10.5	12.949	0.000	0.552	0.000	12.630	0.016
1474	02 00 21.98	+38 02 41.0	10.698	0.009	0.355	0.016	10.441	0.013
1602	02 01 05.97	+37 42 23.6	9.961	0.011	0.462	0.014	9.671	0.013
							8.978	0.020
							8.786	0.032
							8.733	0.023